

LEARNING SPARSE MASKS FOR DIFFUSION-BASED IMAGE INPAINTING

Tobias Alt, Pascal Peter, and Joachim Weickert

Mathematical Image Analysis Group, Faculty of Mathematics and Computer Science,
Campus E1.7, Saarland University, 66041 Saarbrücken, Germany.
{alt, peter, weickert}@mia.uni-saarland.de

ABSTRACT

Diffusion-based inpainting is a powerful tool for the reconstruction of images from sparse data. Its quality strongly depends on the choice of known data. Optimising their spatial location – the inpainting mask – is challenging. A commonly used tool for this task are stochastic optimisation strategies. However, they are slow as they compute multiple inpainting results. We provide a remedy in terms of a learned mask generation model. By emulating the complete inpainting pipeline with two networks for mask generation and neural surrogate inpainting, we obtain a model for highly efficient adaptive mask generation. Experiments indicate that our model can achieve competitive quality with an acceleration by as much as four orders of magnitude. Our findings serve as a basis for making diffusion-based inpainting more attractive for various applications such as image compression, where fast encoding is highly desirable.

Index Terms— Image Inpainting, Diffusion, Partial Differential Equations, Data Optimisation, Deep Learning

1. INTRODUCTION

Inpainting is the task of restoring an image from limited amounts of data. Diffusion-based inpainting is particularly powerful for reconstructions from sparse data; see e.g. [1]. By solving a partial differential equation (PDE), it propagates information from a small known subset of pixels, the inpainting mask, to the missing image areas. Inpainting from sparse data has been successful in various applications such as image compression [2, 3, 4], adaptive sampling [5], and denoising [6].

Optimising the inpainting mask is integral for a good reconstruction. However, this is a challenging combinatorial problem. While there are theoretical results on optimal masks [7], practical implementations are often not convincing albeit highly efficient. On the other hand, stochastic mask optimisation strategies [8] produce high quality masks, but are computationally expensive.

In the present paper, we combine efficiency and quality of mask optimisation for PDE-based inpainting with the help of deep learning. To this end, we design a hybrid architecture which, to the best of our knowledge, constitutes the first instance of learned sparse masks for PDE-based inpainting.

1.1. Our Contribution

We present a model for learning sparse inpainting masks for homogeneous diffusion inpainting. This type of inpainting shows good

performance for optimised masks [8], and does not depend on any free parameters. We employ two networks: one which generates a sparse inpainting mask, and one which acts as a surrogate solver for homogeneous diffusion inpainting. By using different loss functions for the two networks, we optimise both inpainting quality and fidelity to the inpainting equation.

The use of a surrogate solver is a crucial novelty in our work. It reproduces results of a diffusion-based inpainting process without having to perform backpropagation through iterations of a numerical solver. This replicates the full inpainting pipeline to efficiently train a mask optimisation model.

We then evaluate the quality of the learned masks in a learning-free inpainting setting. Our model combines the speed of instantaneous mask generation approaches [7] with the quality of stochastic optimisation [8]. Thus, we reach a new milestone in sparse mask optimisation for diffusion-based inpainting.

1.2. Related Work

Diffusion-based inpainting (see e.g. [1]) plays a vital role in image and video compression [2, 3, 9], denoising [6], and many more.

A good inpainting mask is crucial for successful image inpainting. In the continuous setting, Belhachmi et al. [7] have shown that optimal masks for homogeneous diffusion inpainting can be obtained from the Laplacian magnitude of the image. However, in practice it is difficult to transfer the continuous optimality to high quality results on discrete images. Still, this approach can be very efficient as it does not require to compute any inpainting results. Other works optimise masks with optimal control [10], bi-level optimisation [11], and dithering of error maps [12]. However, these frameworks rely on sophisticated algorithms and require substantial computation time.

A popular tool for mask optimisation was proposed by Mainberger et al. [8]. Their stochastic spatial optimisation strategies rely on successively removing and exchanging random image pixels until a desired number of mask pixels is reached. However, these strategies are slow, in particular for small densities. More recently, Chizhov and Weickert [13] presented an optimisation strategy based on finite elements which alleviates these problems. While being very efficient, their approach still requires to compute the inpainting several times. We develop an alternative in the form of a neural mask generation model. It is able to compete with stochastic masks in terms of quality, without having to compute any inpainting results.

Learning-based inpainting has also been successful in recent years. Following the popular work of Xie et al. [14], several architectures and strategies for inpainting have been proposed; see e.g. [15, 16, 17]. However, inpainting from sparse data is rarely considered. Vařata et al. [18] present sparse inpainting based on Wasserstein generative adversarial networks. Similarly, Ulyanov et al. [19] consider inpainting from sparse data without mask genera-

This work has received funding from the European Research Council (ERC) under the European Union’s Horizon 2020 research and innovation programme (grant agreement no. 741215, ERC Advanced Grant INCOVID).

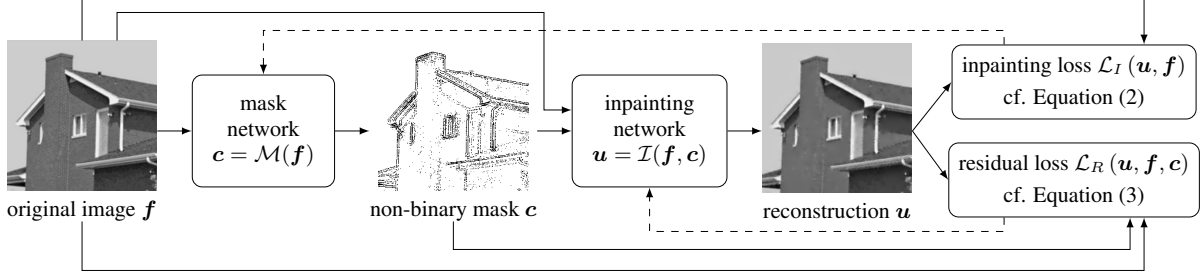


Fig. 1: Overview over our model structure. Solid lines denote forward passes, dashed lines denote backpropagation.

tion. Dai et al. [5] present a trainable mask generation model from an adaptive sampling viewpoint. Our approach is the first to combine deep learning for mask optimisation for PDE-based inpainting in a transparent and efficient way.

1.3. Organisation of the Paper

In Section 2, we briefly review diffusion-based inpainting. Afterwards in Section 3, we introduce our model for learning inpainting masks. We evaluate the quality of the learned masks in Section 4 before presenting our conclusions in Section 5.

2. REVIEW: DIFFUSION-BASED INPAINTING

The goal of inpainting is to restore missing information in an image $f : \Omega \rightarrow \mathbb{R}$ on some rectangular domain Ω , where image data is only available on an inpainting mask $K \subset \Omega$. In this work we focus on homogeneous diffusion inpainting, which computes the reconstruction u as the solution of the PDE

$$(1 - c) \Delta u - c(u - f) = 0 \quad (1)$$

with reflecting boundary conditions. Here, a confidence measure $c : \Omega \rightarrow \mathbb{R}$ denotes whether a value is known or not. Most diffusion-based inpainting models consider binary values for c : A value of $c(x) = 1$ indicates known data and thus $u = f$ on K , while $c(x) = 0$ denotes missing data, leading to homogeneous diffusion [20] inpainting $\Delta u = 0$ on $\Omega \setminus K$ where $\Delta = \partial_{xx} + \partial_{yy}$ denotes the Laplacian. However, it is also possible to use non-binary confidence measures [21], which we will exploit to our advantage.

In practice, one considers digital images $u, f \in \mathbb{R}^{n_x n_y}$ with dimensions $n_x \times n_y$ and discretises the inpainting equation (1) by means of finite differences. Then, a numerical solver is used to obtain a reconstruction u . For a good inpainting quality, optimising the binary mask $c \in \{0, 1\}^{n_x n_y}$ is crucial. This problem is constrained by a desired mask density d which measures the percentage of mask pixels w.r.t. the number of image pixels.

One strategy for mask optimisation has been proposed by Belhachmi et al. [7]. They show that an optimal mask in the continuous setting can be obtained from the rescaled Laplacian magnitude of the image. However, transferring these results to the discrete setting often suffers from suboptimal dithering strategies. While being highly efficient, reconstruction quality is not fully satisfying.

Better quality can be achieved with the popular stochastic strategies of Mainberger et al. [8]. First, one employs *probabilistic sparsification* (PS): Starting with a full mask, one removes a fraction p of candidate pixels and computes the inpainting. Then, one reintroduces a fraction q of the candidates with the largest local inpainting error. One repeats this step until reaching a desired mask density d .

Since sparsification is a greedy local approach, it can get trapped in bad local minima. As a remedy, Mainberger et al. [8] also propose a *nonlocal pixel exchange* (NLPE). Pixel candidates in a sparsified mask are exchanged for an equally large set of non-mask pixels. If the new inpainting result improves, the exchange is kept, otherwise it is discarded. In theory, NLPE can only improve the mask, but in practice convergence is slow.

The use of PS and NLPE requires to solve the inpainting problem numerous times, leading to slow mask optimisation. To avoid this computational bottleneck, we want to reach the quality of stochastic mask optimisation with a more efficient model based on deep learning.

3. SPARSE MASKS WITH SURROGATE INPAINTING

Our model consists of two equally shaped U-nets [22] with different loss functions. By optimising both inpainting quality and fidelity to the inpainting equation, we obtain masks with good reconstruction quality for the inpainting problem at hand.

3.1. The Mask Network

The *mask network* takes an original image f and transforms it into a mask c . We denote the forward pass through the mask network by $\mathcal{M}(\cdot)$, i.e. the mask is computed as $c = \mathcal{M}(f)$.

The mask entries lie in the interval $[0, 1]$. Permitting non-binary values allows for a differentiable network model. To obtain mask points in the desired range, we apply a sigmoid function to the output of the network. Moreover, the mask network is trained for a specific mask density d . To this end, we rescale the outputs of the network if they exceed the desired density. We do not require a lower bound, since the loss function incites a sufficiently dense mask.

The mask network chooses the known data such that the inpainting error of the corresponding reconstruction u w.r.t. the original f is minimised. This yields the *inpainting loss*

$$\mathcal{L}_I(u, f) = \frac{1}{n_x n_y} \|u - f\|_2^2 \quad (2)$$

as its objective function. Its implicit dependency on the inpainting mask links the learned masks to the reconstructions.

We found that the mask network tends to get stuck in local minima with flat masks. To avoid this, we add a regularisation term $\mathcal{R}(c)$ to the inpainting loss $\mathcal{L}_I(u, f)$. It penalises the inverse variance of the mask via $\mathcal{R}(c) = (\sigma_c^2 + \epsilon)^{-1}$ where a small constant ϵ avoids division by zero. The regulariser serves two purposes: First, it lifts the bad local minima for flat masks by adding a strong penalty to the energy landscape. Secondly, it promotes masks with values closer to



Fig. 2: Test images of resolution 256×256 .

0 and 1, as this maximises the variance. The impact of the regularisation term is steered by a positive regularisation parameter α .

3.2. The Inpainting Network

The second network is called the *inpainting network*. Its task is to create a reconstruction \mathbf{u} which follows a classical inpainting process. In [23], it has been shown that U-nets realise an efficient multi-grid strategy at their core. Thus, we use a U-net as a surrogate solver which reproduces the results of the PDE-based inpainting. The inpainting network takes the original image \mathbf{f} and the mask \mathbf{c} and creates a reconstruction $\mathbf{u} = \mathcal{I}(\mathbf{f}, \mathbf{c})$. It minimises the residual of the inpainting equation (1). This yields the *residual loss*

$$\mathcal{L}_R(\mathbf{u}, \mathbf{f}, \mathbf{c}) = \frac{1}{n_x n_y} \|(\mathbf{I} - \mathbf{C}) \mathbf{A}(\mathbf{u})\mathbf{u} - \mathbf{C}(\mathbf{u} - \mathbf{f})\|_2^2. \quad (3)$$

Here, $\mathbf{A}(\mathbf{u})$ is a discrete implementation of the Laplacian Δ with reflecting boundary conditions, and $\mathbf{C} = \text{diag}(\mathbf{c})$ is a matrix representation of the mask.

As the residual loss measures fidelity to the PDE-based process, an optimal network approximates the PDE solution in an efficient way that allows fast backpropagation. This strategy has been proposed in [23] and is closely related to the idea of deep energies [24].

Figure 1 presents an overview of the full model structure. Note that the inpainting network receives both the mask and the original image as an input. Thus, this network is not designed for standalone inpainting. However, this allows the network to easily minimise the residual loss by transforming the original into an accurate inpainting result, given the mask as side information.

3.3. Practical Application

After training the full pipeline in a joint fashion, the mask network can be used to generate masks for homogeneous diffusion inpainting. To this end, we apply the mask network to an original image and obtain a non-binary mask. This mask is then binarised by a sampling: The probability of a pixel belonging to a mask is given by its non-binary value. At each position, we perform a weighted coin flip with that probability. Afterwards, the binarised masks are fed into a numerical solver of choice for homogeneous diffusion inpainting.

While binarising the mask is not necessary in this pure inpainting framework, it is important for compression applications since storing binary masks with arbitrary point distributions is already highly non-trivial [25].

4. EXPERIMENTS

4.1. Experimental Setup

We train both U-nets jointly with their respective loss function on the BSDS500 dataset [26]. As a training set, we use 200 cropped grey value images of size 256×256 with values in the range $[0, 255]$.

Both U-nets employ 5 scales, with 3 layers per scale. On the finest scale, they use 10 channels, and this number is doubled on each scale. Thus, each U-net possesses around 9×10^5 parameters. We use the Adam optimiser [27] with standard settings, a learning rate of $5 \cdot 10^{-4}$, and 4000 epochs. As a regularisation parameter we choose $\alpha = 0.01$. We train multiple instances of the model for densities between 10% and 1% with several random initialisations.

After training, we binarise the masks and use them with a conjugate gradient solver for homogeneous diffusion inpainting to obtain a reconstruction. Since we aim at the highest quality, we take the best result out of 30 samplings.

Analogously, we generate masks with PS and PS with additional NLPE. In the following, we denote the latter combination by PS+NLPE. In our sparsification we use candidate fractions $p = 0.1$ and $q = 0.05$, and we take the best result out of 5 runs. For NLPE, we use 30 candidates of which 10 are exchanged. We run NLPE for 10 cycles. In a single cycle, each mask point is exchanged once on average. Moreover, we compare against the strategy of Belhachmi et al. [7]. This approach is realised by taking the Laplacian magnitude of the image, rescaling it to obtain a desired density, and dithering the result with a binary Floyd–Steinberg algorithm [28].

We compare our results on five popular test images (see Figure 2), since performing PS and NLPE on a large database is infeasible. We measure the quality in terms of peak signal-to-noise ratio (PSNR). Higher values indicate better quality.

4.2. Reconstruction Quality

Figure 3 shows a visual comparison of optimised masks and the corresponding inpainting results. For both test cases, we observe that our learned masks are structurally similar to those obtained by PS with NLPE. This helps to create sharper contours, whereas the inpainting results of Belhachmi et al. suffer from fuzzy edges. The visual quality of the inpainting results for our model and PS+NLPE is indeed competitive.

Figure 4 presents a comparison of the reconstruction quality averaged over the test images. Our learned masks consequently outperform the strategy of Belhachmi et al.. Moreover, our model is on par with PS for densities smaller than 5%. For extremely small densities up to 2%, it even outperforms PS and is on par with PS+NLPE.

For larger mask densities, the differences between the methods become smaller, and our model cannot outperform its stochastic counterparts. Still, all approaches produce a good reconstruction quality. However, for applications such as inpainting-based image compression, very sparse masks are more important and more challenging [3, 8]. Therefore, our mask generation model performs well for the practically relevant mask densities.

4.3. Computational Efficiency

The big advantage of the learned mask generation is its speed. As inpainting operations are the dominant factor for computation time, we use the number of inpaintings as a measure for efficiency. In comparison, the forward pass of the mask network is negligible.

Figure 5 visualises the average number of inpaintings required to obtain masks of a specific density for the test set. To generate a mask, both our model and that of Belhachmi et al. do not require any inpainting operations. Thus, the efficiency of these mask generation strategies does not depend on the density.

For PS, lower densities require more inpainting operations. Adding NLPE requires even more inpainting operations depending

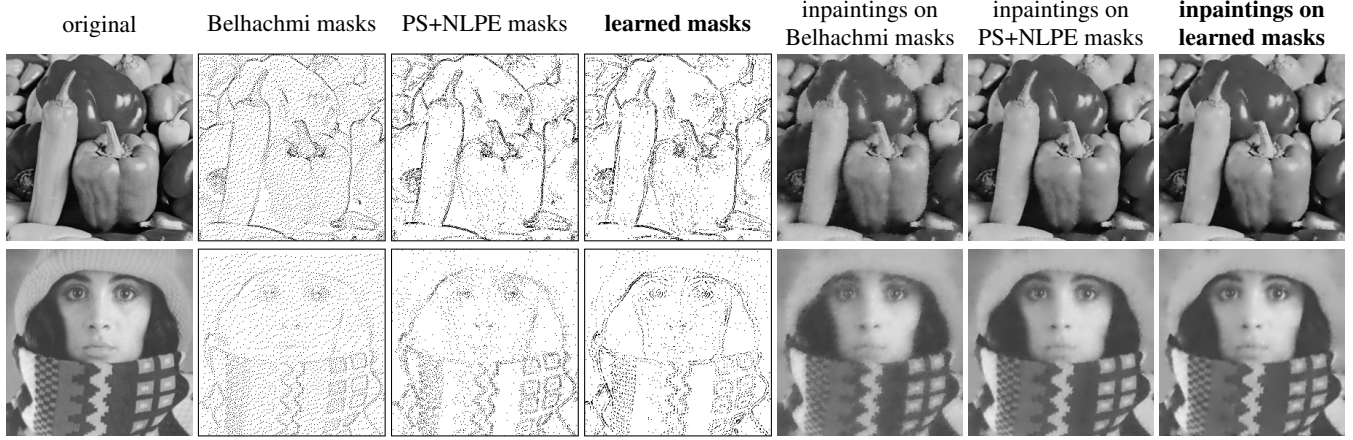


Fig. 3: Visual comparison of inpainting results on two exemplary images for different mask densities. Mask points are shown in black, and mask images are framed for better visibility. **Top row:** Results on *peppers* for 8% density. **Bottom row:** Results on *trui* for 5% density. The learned masks yield inpainting results which are visually comparable to PS with additional NLPE.

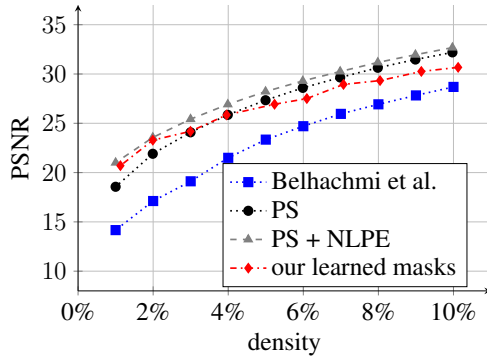


Fig. 4: Comparison of average inpainting quality on the test images. The learned masks consistently outperform those of Belhachmi et al. and can compete with masks generated by PS. For very sparse masks, our model can compete with PS+NLPE.

on the number of cycles and the mask density. Both strategies trade computational efficiency for inpainting quality.

For example, one sparsification run for a 3% mask on the *cameraman* image with realistic parameter settings requires 700 steps. The additional NLPE optimisation requires another 2000 steps. In total, this single mask optimisation requires 2700 inpaintings.

Our learned mask generation is as fast as the strategy of Belhachmi et al., while being on par with the stochastic optimisation in terms of quality. This allows instantaneous high quality mask generation. As a consequence, our learned model can serve as a highly efficient replacement of stochastic mask optimisation.

5. CONCLUSIONS

Our approach combines ideas from deep learning with classical modelling of diffusion-based inpainting. The key of this strategy is a combination of an inpainting loss for the mask generator and a residual loss for the surrogate inpainting network.

The proposed model is the first instance of learned sparse masks for diffusion-based inpainting. Its results are competitive with stochastic mask optimisation, while being up to four orders of mag-

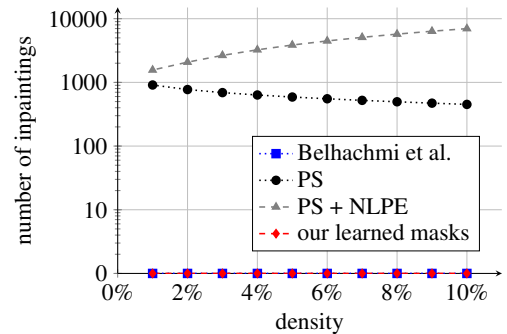


Fig. 5: Comparison of efficiency in terms of the number of inpaintings for each density. Both our method and that of Belhachmi et al. generate masks without computing an inpainting. The stochastic optimisation strategies compute up to thousands of inpaintings.

nitude faster. This constitutes a new milestone in mask optimisation for diffusion-based inpainting.

We are currently extending this idea to more sophisticated inpainting operators, as well as optimising the network architecture to fully outperform the stochastic optimisation strategies. We hope that this paves the way for combining quality and efficiency for diffusion-based inpainting and its applications.

6. REFERENCES

- [1] J. Weickert and M. Welk, “Tensor field interpolation with PDEs,” in *Visualization and Processing of Tensor Fields*, J. Weickert and H. Hagen, Eds., pp. 315–325. Springer, Berlin, 2006.
- [2] I. Galić, J. Weickert, M. Welk, A. Bruhn, A. Belyaev, and H.-P. Seidel, “Image compression with anisotropic diffusion,” *Journal of Mathematical Imaging and Vision*, vol. 31, no. 2–3, pp. 255–269, July 2008.
- [3] C. Schmaltz, P. Peter, M. Mainberger, F. Ebel, J. Weickert, and A. Bruhn, “Understanding, optimising, and extending data compression with anisotropic diffusion,” *International Journal of Computer Vision*, vol. 108, no. 3, pp. 222–240, July 2014.

- [4] P. Peter, S. Hoffmann, F. Nedwed, L. Hoeltgen, and J. Weickert, "Evaluating the true potential of diffusion-based inpainting in a compression context," *Signal Processing: Image Communication*, vol. 46, pp. 40–53, Aug. 2016.
- [5] Q. Dai, H. Chopp, E. Pouyet, O. Cossairt, M. Walton, and A. K. Katsaggelos, "Adaptive image sampling using deep learning and its application on X-Ray fluorescence image reconstruction," *IEEE Transactions on Multimedia*, vol. 22, no. 10, pp. 2564–2578, Dec. 2019.
- [6] R. D. Adam, P. Peter, and J. Weickert, "Denoising by inpainting," in *Scale Space and Variational Methods in Computer Vision*, F. Lauze, Y. Dong, and A. B. Dahl, Eds., vol. 10302 of *Lecture Notes in Computer Science*, pp. 121–132. Springer, Cham, 2017.
- [7] Z. Belhachmi, D. Bucur, B. Burgeth, and J. Weickert, "How to choose interpolation data in images," *SIAM Journal on Applied Mathematics*, vol. 70, no. 1, pp. 333–352, 2009.
- [8] M. Mainberger, S. Hoffmann, J. Weickert, C. H. Tang, D. Johannsen, F. Neumann, and B. Doerr, "Optimising spatial and tonal data for homogeneous diffusion inpainting," in *Scale Space and Variational Methods in Computer Vision*, A. M. Bruckstein, B. ter Haar Romeny, A. M. Bronstein, and M. M. Bronstein, Eds., vol. 6667 of *Lecture Notes in Computer Science*, pp. 26–37. Springer, Berlin, 2012.
- [9] S. Andris, P. Peter, R. M. K. Mohideen, J. Weickert, and S. Hoffmann, "Inpainting-based video compression in FullHD," in *Scale Space and Variational Methods in Computer Vision*, A. Elmoataz, J. Fadili, Y. Quéau, J. Rabin, and L. Simon, Eds., vol. 12679 of *Lecture Notes in Computer Science*, pp. 425–436. Springer, Cham, 2021.
- [10] L. Hoeltgen, S. Setzer, and J. Weickert, "An optimal control approach to find sparse data for Laplace interpolation," in *Energy Minimisation Methods in Computer Vision and Pattern Recognition*, A. Heyden, F. Kahl, C. Olsson, M. Oskarsson, and X.-C. Tai, Eds., vol. 8081 of *Lecture Notes in Computer Science*, pp. 151–164. Springer, Berlin, 2013.
- [11] Y. Chen, R. Ranftl, and T. Pock, "A bi-level view of inpainting-based image compression," in *Proc. 19th Computer Vision Winter Workshop*, Z. Kúkelová and J. Heller, Eds., Křtiny, Czech Republic, Feb. 2014.
- [12] L. Karos, P. Bheed, P. Peter, and J. Weickert, "Optimising data for exemplar-based inpainting," in *Advanced Concepts for Intelligent Vision Systems*, J. Blanc-Talon, D. Helbert, W. Philips, D. Popescu, and P. Scheunders, Eds., vol. 11182 of *Lecture Notes in Computer Science*, pp. 547–558. Springer, Cham, 2018.
- [13] V. Chizhov and J. Weickert, "Efficient data optimisation for harmonic inpainting with finite elements," arXiv:2105.01586 [eess.IV], May 2021, To appear in N. Tsapatsoulis, A. Panayides, T. Theo, A. Lanitis, C. Pattichis (Eds.): *Computer Analysis of Images and Patterns. Lecture Notes in Computer Science*, Springer, Cham, 2021.
- [14] J. Xie, L. Xu, and E. Chen, "Image denoising and inpainting with deep neural networks," in *Proc. 26th International Conference on Neural Information Processing Systems*, P. L. Bartlett, F. C. N. Pereira, C. J. C. Burges, L. Bottou, and K. Q. Weinberger, Eds., Lake Tahoe, NV, Dec. 2012, vol. 25 of *Advances in Neural Information Processing Systems*, pp. 350–358.
- [15] D. Pathak, P. Krähenbühl, J. Donahue, T. Darrell, and A. A. Efros, "Context encoders: Feature learning by inpainting," in *Proc. 2016 IEEE Conference on Computer Vision and Pattern Recognition*, Las Vegas, NV, June 2016, pp. 2536–2544.
- [16] C. Yang, X. Lu, Z. Lin, E. Shechtman, O. Wang, and H. Li, "High-resolution image inpainting using multi-scale neural patch synthesis," in *Proc. 2017 IEEE Conference on Computer Vision and Pattern Recognition*, Honolulu, HI, July 2017, pp. 6721–6729.
- [17] J. Yu, Z. Lin, J. Yang, X. Shen, X. Lu, and T. S. Huang, "Generative image inpainting with contextual attention," in *Proc. 2018 IEEE Conference on Computer Vision and Pattern Recognition*, Salt Lake City, UT, June 2018, pp. 5505–5514.
- [18] D. Vařata, T. Halama, and M. Friedjungová, "Image inpainting using Wasserstein generative adversarial imputation network," in *Artificial Neural Networks and Machine Learning – ICANN 2021*, I. Farkaš, P. Masulli, S. Otte, and S. Wermter, Eds., vol. 12892 of *Lecture Notes in Computer Science*, pp. 575–586. Springer, Cham, 2021.
- [19] D. Ulyanov, A. Vedaldi, and V. Lempitsky, "Deep image prior," in *Proc. 2018 IEEE Conference on Computer Vision and Pattern Recognition*, Salt Lake City, UT, June 2018, pp. 9446–9454.
- [20] T. Iijima, "Basic theory on normalization of pattern (in case of typical one-dimensional pattern)," *Bulletin of the Electrotechnical Laboratory*, vol. 26, pp. 368–388, 1962, In Japanese.
- [21] L. Hoeltgen and J. Weickert, "Why does non-binary mask optimisation work for diffusion-based image compression?," in *Energy Minimisation Methods in Computer Vision and Pattern Recognition*, X.-C. Tai, E. Bae, T. F. Chan, S. Y. Leung, and M. Lysaker, Eds., vol. 8932 of *Lecture Notes in Computer Science*, pp. 85–98. Springer, Berlin, 2015.
- [22] O. Ronneberger, P. Fischer, and T. Brox, "U-net: Convolutional networks for biomedical image segmentation," in *Medical Image Computing and Computer-Assisted Intervention – MICCAI 2015*, N. Navab, J. Hornegger, W. Wells, and A. Frangi, Eds., vol. 9351 of *Lecture Notes in Computer Science*, pp. 234–241. Springer, Cham, 2015.
- [23] T. Alt, K. Schrader, M. Augustin, P. Peter, and J. Weickert, "Connections between numerical algorithms for PDEs and neural networks," arXiv:2107.14742v1 [math.NA], July 2021.
- [24] A. Golts, D. Freedman, and M. Elad, "Deep energy: Task driven training of deep neural networks," *IEEE Journal of Selected Topics in Signal Processing*, vol. 15, no. 2, pp. 324–338, Feb. 2021.
- [25] R. M. K. Mohideen, P. Peter, and J. Weickert, "A systematic evaluation of coding strategies for sparse binary images," *Signal Processing: Image Communication*, vol. 99, pp. Article no. 116424, Nov. 2021.
- [26] P. Arbelaez, M. Maire, C. Fowlkes, and J. Malik, "Contour detection and hierarchical image segmentation," *IEEE Transactions on Pattern Analysis and Machine Intelligence*, vol. 33, no. 5, pp. 898–916, Aug. 2011.
- [27] D. P. Kingma and J. Ba, "Adam: A method for stochastic optimization," arXiv:1412.6980v1 [cs.LG], Dec. 2014.
- [28] R. W. Floyd and L. Steinberg, "An adaptive algorithm for spatial grey scale," *Proceedings of the Society of Information Display*, vol. 17, pp. 75–77, 1976.